Research Square

Preprints are preliminary reports that have not undergone peer review.
They should not be considered conclusive, used to inform clinical practice,
or referenced by the media as validated information.

# Paired liver–spleen profiling links Marek's disease virus burden to tissue-specific cytokine remodeling in naturally infected chickens

**Sumaiya Salim Tasnim**
Chattogram Veterinary and Animal Sciences University
**Farjana Akter**
Chattogram Veterinary and Animal Sciences University
**Mahabub Alam**
Chattogram Veterinary and Animal Sciences University
**Lipi Akter**
Kagoshima University
**Md Jahedul Hasan Rocky**
Chattogram Veterinary and Animal Sciences University
**Md Moksedul Momin**
The University of Queensland
**Sharmin Chowdhury**
Chattogram Veterinary and Animal Sciences University
**Md Masuduzzaman**
Chattogram Veterinary and Animal Sciences University
**Tofazzal Md Rakib**
rakibtofazzal@cvasu.ac.bd

Chattogram Veterinary and Animal Sciences University

**Article**

**Keywords:** Marek's disease virus, cytokines, viral burden, liver, spleen, mixed-effects model

**Posted Date:** September 8th, 2026

**DOI:** https://doi.org/10.21203/rs.3.rs-10777412/v1

**License:** This work is licensed under a Creative Commons Attribution 4.0 International License. Read Full License

**Additional Declarations:** No competing interests reported.

## Abstract

Marek's disease virus (MDV), a highly contagious, immunosuppressive, and oncogenic virus of chickens, yet tissue-level relationships between viral burden and cytokine responses remain poorly defined. This study quantified MDV genomic load and cytokines such as *IFN-γ*, *IL-2*, *IL-4*, *IL-6*, *IL-10*, and *IL-17* expression in paired liver and spleen samples from naturally infected chickens and MDV-negative controls. MDV was confirmed by *ICP4*-targeted PCR, viral burden was measured by quantitative PCR as genome copies per nanogram (ng) of extracted DNA, and cytokine expression was assessed by GAPDH-normalized RT-qPCR. Eighteen MDV-positive birds had complete paired measurements. Mean viral burden was higher in liver than spleen, but the paired difference was not significant. Mixed-effects modelling, with tissue as a fixed effect and bird identity as a random intercept, showed that increasing viral burden was associated with reduced *IFN-γ* and *IL-2* expression and increased *IL-4*, *IL-6*, *IL-10*, and *IL-17* expression. *IL-10* exhibited the largest proportional increase, while no viral burden-by-tissue interaction remained significant after multiple-testing correction. Overall, increasing MDV burden was associated with reduced antiviral cytokine responses and enhanced inflammatory and immunoregulatory activity, indicating coordinated immune remodeling across liver and spleen and providing insight into MDV pathogenesis and host responses during natural infection.

## Introduction

Marek's disease (MD) is a highly contagious, immunosuppressive, and oncogenic disease of chickens caused by Marek's disease virus (MDV), classified within the species *Mardivirus gallidalpha2* and formerly designated *Gallid alphaherpesvirus 2*. The disease is characterized by peripheral nerve lesions, visceral T-cell lymphomas, immunosuppression, production losses, and mortality. Although vaccination has markedly reduced the incidence of clinical disease, currently available vaccines do not induce sterilizing immunity and therefore do not completely prevent infection, viral replication, or shedding. Continued circulation of MDV in vaccinated flocks consequently remains a major challenge to poultry health and may contribute to the persistence and evolution of highly virulent field strains [1, 2].

Transmission occurs predominantly through inhalation of contaminated feather dander and poultry-house dust. Fully infectious virions are produced during productive replication in feather follicle epithelial cells and are shed with feather debris and dander, which can remain infectious in the environment for months and facilitate efficient horizontal transmission [3, 4]. Following respiratory entry, MDV can infect macrophages, which may contribute to viral transport from the respiratory tract to lymphoid tissues. The virus subsequently undergoes an early cytolytic phase involving primarily B lymphocytes in the bursa of Fabricius, thymus, and spleen. This phase is associated with apoptosis, lymphoid depletion, inhibition of cellular proliferation, and marked immunosuppression [5–7]. MDV then establishes latency predominantly in activated $CD4^+$ T lymphocytes, a proportion of which may undergo neoplastic transformation. The MDV-encoded Meq oncoprotein is central to this process and is required for lymphoma formation, although it is not essential for productive viral replication [8, 9].

Quantification of the MDV genome provides an important measure of infection intensity, tissue distribution, and disease-associated viral burden. MDV DNA can be detected in blood lymphocytes, spleen, liver, feather follicles, and other tissues, although its abundance varies with viral pathotype, host genotype, vaccination status, tissue type, and infection stage [10–12]. The spleen is a major lymphoid site of early replication, immune activation, latency, and reactivation, whereas the liver is frequently involved in systemic dissemination, inflammatory infiltration, and visceral lymphoma development. However, paired assessment of viral burden and local immune responses in liver and spleen from the same naturally affected birds remain limited.

Cytokine responses are important determinants of both antiviral protection and MDV-associated immunopathology. *IFN-γ* and *IL-2* support Th1-type cellular immunity, macrophage activation, and T-cell proliferation, and experimental evidence indicates that interferons can restrict MDV replication and delay disease progression [13, 14]. Conversely, MDV infection can induce *IL-4*, *IL-6*, *IL-10*, and other inflammatory or immunoregulatory cytokines, indicating complex immune remodeling during cytolytic infection, persistence, and tumor development [15, 16]. *IL-10* may facilitate immune evasion by limiting antigen presentation and Th1-associated responses, whereas *IL-17* may contribute to inflammatory recruitment or compensatory antiviral activity depending on the stage and immunological context of infection [17]. Furthermore, MDV-specific T cells may proliferate and

express antiviral cytokines while displaying impaired degranulation, demonstrating that cytokine transcription does not necessarily correspond to effective viral clearance [17].

Accordingly, the present study quantified MDV genomic burden and evaluated the expression of *IFN-γ*, *IL-2*, *IL-4*, *IL-6*, *IL-10*, and *IL-17* in paired liver and spleen samples from MDV-negative control and naturally affected chickens. Viral burden was assessed primarily as a continuous variable, while a study-specific median systemic-burden index was used only for descriptive grouping. Cytokine–viral burden relationships and tissue-specific effects were evaluated using mixed-effects models that accounted for paired observations within individual birds. This integrated approach aimed to characterize burden-associated immune-expression patterns and improve understanding of tissue-level host–virus interactions during naturally occurring MDV infection.

## Results

### Tissue distribution of MDV

Among the chickens included in the quantitative analysis, 18 MDV-positive birds had complete paired liver and spleen measurements, whereas MDV was non-detectable in the five control birds. Considerable interindividual variation in viral burden was observed in both tissues. Mean MDV burden was 14,355.64 copies/ng of extracted DNA in the liver and 6,935.13 copies/ng in the spleen. The corresponding median values were 3,661.15 and 1,669.49 copies/ng DNA, respectively. Liver viral burden ranged from 50.50 to 86,816.36 copies/ng DNA, whereas spleen burden ranged from 22.79 to 51,555.87 copies/ng DNA. Although the average viral burden was numerically higher in the liver, paired comparison of $\log_{10}$-transformed copy numbers showed no statistically significant difference between liver and spleen samples (Wilcoxon signed-rank statistic = 51.0, $P = 0.139$; Figure 1). Individual paired trajectories were heterogeneous, with some birds showing higher viral burden in the liver and others showing higher burden in the spleen.

The systemic MDV-burden index, calculated as the geometric mean of the paired liver and spleen loads, ranged from 91.60 to 35,484.40 copies/ng DNA. The median systemic burden was 2,983.54 copies/ng DNA. For descriptive visualization, the 18 MDV-positive birds were therefore divided into lower- and higher-burden groups containing nine birds each. This classification was study-specific and was not interpreted as a diagnostic or disease-stage threshold.

### Cytokine-expression patterns according to systemic MDV burden

GAPDH-normalized expression of the six cytokines differed according to systemic MDV-burden category, although the magnitude and statistical strength of the differences varied between tissues (Figure 2). In the liver, significant overall group differences were detected for *IL-2* ($q = 0.012$), *IL-4* ($q = 0.003$), *IL-6* ($q = 0.003$), *IL-10* ($q = 0.003$), and *IL-17* ($q = 0.004$). The overall difference in hepatic *IFN-γ* expression did not remain statistically significant after correction for multiple testing ($q = 0.065$).

In the spleen, significant overall group effects were identified for all evaluated cytokines, including *IFN-γ* ($q = 0.006$), *IL-2* ($q = 0.013$), *IL-4* ($q = 0.003$), *IL-6* ($q = 0.003$), *IL-10* ($q = 0.003$), and *IL-17* ($q = 0.006$). The distributions generally indicated lower *IFN-γ* and *IL-2* expression in the higher-burden group, accompanied by progressively higher *IL-4*, *IL-6*, *IL-10*, and *IL-17* expression. These comparisons represent omnibus group effects; specific pairwise differences were not inferred from the Kruskal–Wallis tests alone.

### Tissue-specific correlations between MDV burden and cytokine expression

Among MDV-positive birds, liver viral burden was significantly associated with all six cytokines after Benjamini–Hochberg correction (Figure 3). Increasing hepatic MDV burden was inversely correlated with *IFN-γ* (Spearman's $\rho = -0.707$, $q = 0.0025$) and *IL-2* ($\rho = -0.775$, $q = 0.0010$). In contrast, positive correlations were observed for *IL-4* ($\rho = 0.779$, $q = 0.0010$), *IL-6* ($\rho = 0.624$, $q = 0.0096$), *IL-10* ($\rho = 0.761$, $q = 0.0010$), and *IL-17* ($\rho = 0.732$, $q = 0.0017$).

In the spleen, MDV burden was negatively correlated with *IFN-γ* (ρ = −0.680, *q* = 0.0038) and *IL-2* (ρ = −0.507, *q* = 0.0425) and positively correlated with *IL-6* (ρ = 0.523, *q* = 0.0388). Associations with *IL-4* (ρ = 0.323, *q* = 0.208), *IL-10* (ρ = 0.377, *q* = 0.148), and *IL-17* (ρ = 0.162, *q* = 0.521) were not significant after multiple-testing correction. Thus, continuous viral burden showed a broader and more consistent relationship with cytokine expression in the liver than in the spleen.

**Tissue-resolved cytokine-expression profiles**

The tissue-resolved heatmap further illustrated the relationship between systemic viral burden and cytokine expression across individual MDV-positive birds (Figure 4). Rows were ordered from lower to higher systemic burden, and expression was standardized separately for each cytokine and tissue. Lower-burden birds generally showed relatively higher *IFN-γ* and *IL-2* expression and lower *IL-4*, *IL-6*, *IL-10*, and *IL-17* expression. In contrast, many higher-burden birds showed reduced antiviral cytokine expression together with increased inflammatory and regulatory cytokine expression. The pattern was more consistent in the liver, particularly for *IL-4*, *IL-6*, *IL-10*, and *IL-17*. Nevertheless, substantial interindividual and tissue-specific heterogeneity remained evident, and paired liver and spleen samples from the same bird did not always exhibit identical standardized expression profiles.

**Mixed-effects associations between viral burden and cytokine expression**

Linear mixed-effects models were used to evaluate cytokine associations with continuous MDV burden while accounting for paired liver and spleen measurements within individual birds. All six models converged successfully. After adjustment for tissue and between-bird variability, increasing MDV burden remained significantly associated with each cytokine evaluated (Table 2; Figure 5).

For every 10-fold increase in MDV copies/ng DNA, *IFN-γ* expression decreased to 0.817-fold of its previous level (95% CI: 0.727–0.918; *q* = 0.0018), corresponding to an estimated 18.3% reduction. *IL-2* expression decreased to 0.837-fold (95% CI: 0.775–0.904; *q* < 0.001), corresponding to a 16.3% reduction. Conversely, each 10-fold increase in MDV burden was associated with a 1.372-fold increase in *IL-4* expression (95% CI: 1.139–1.653; *q* = 0.0018), a 1.247-fold increase in *IL-6* expression (95% CI: 1.089–1.429; *q* = 0.0018), a 1.527-fold increase in *IL-10* expression (95% CI: 1.230–1.896; *q* = 0.0012), and a 1.319-fold increase in *IL-17* expression (95% CI: 1.072–1.624; *q* = 0.012). *IL-10* therefore showed the largest proportional positive association with increasing viral burden.

No MDV-burden-by-tissue interaction remained statistically significant after correction for multiple testing, with adjusted interaction *q*-values ranging from 0.173 to 0.569. The common-slope models were therefore retained, indicating that the overall directions of the viral load–cytokine relationships were broadly comparable between liver and spleen. Bird-level intraclass correlation coefficients ranged from 0.217 to 0.739, demonstrating appreciable within-bird dependence and supporting the inclusion of bird identity as a random effect.

# Discussion

The present study combined paired liver–spleen quantification of Marek's disease virus (MDV) with cytokine-expression profiling to examine how tissue viral burden relates to local immune responses in naturally affected chickens. Three findings were prominent: MDV burden varied markedly among birds but did not differ consistently between paired liver and spleen samples; increasing viral burden was associated with reduced *IFN-γ* and *IL-2* expression and increased *IL-4*, *IL-6*, *IL-10*, and *IL-17* expression; and these associations remained evident in mixed-effects models accounting for paired tissues within birds. The absence of a significant burden-by-tissue interaction suggests that the overall direction of the associations was broadly similar in both organs, although the modest sample size limits the power to detect smaller tissue-specific effects.

The presence of MDV in both tissues is consistent with systemic viral dissemination. Experimental studies have detected MDV genomes in blood lymphocytes, spleen, liver, feather follicles, and other organs, with viral quantity varying according to tissue, viral strain, host genotype, and infection stage [10–12]. [11] reported comparatively high viral quantities in lymphocytes, liver, and spleen, with the greatest burden in feather follicles. In the present study, mean viral burden was numerically higher in the

liver, but paired comparison did not support a consistent organ-level difference. A non-significant result does not establish equivalence; instead, it indicates that liver–spleen differences varied among birds. This heterogeneity may reflect lesion distribution, lymphocyte trafficking, tumor involvement, or sampling relative to cytolytic replication, latency, reactivation, and neoplastic progression.

Continuous analysis of $\log_{10}$-transformed MDV copies/ng DNA was therefore more informative than classification using a fixed biological cutoff. The study-specific systemic burden index and median split were useful for descriptive presentation but should not be interpreted as diagnostic thresholds or direct indicators of latent and clinical infection. Published MDV qPCR studies differ in target genes, calibration standards, tissue matrices, and reporting denominators; some normalize viral genomes to a host single-copy gene, whereas the present study expressed viral burden per nanogram of extracted DNA [11, 12]. Although normalization to DNA mass standardizes template input, it does not directly account for tissue cellularity or the number of host-cell equivalents. Future studies should therefore consider duplex quantification using a validated single-copy chicken genomic target.

The inverse associations of *IFN-γ* and *IL-2* with viral burden are biologically plausible in established field infection but must be interpreted according to infection stage. *IFN-γ* is induced during early MDV infection and has been associated with increasing splenic viral load during the acute response [13]. A positive relationship between MDV replication and *IFN-γ* expression has also been observed in feathers, suggesting that early *IFN-γ* induction may reflect active immune recognition rather than successful viral control [18]. Experimental evidence further demonstrates that IFN-α and *IFN-γ* can inhibit MDV replication and delay disease progression [14]. Therefore, lower *IFN-γ* expression at greater viral burden in the present study may represent failure, exhaustion, or suppression of antiviral immunity during persistent or advanced disease rather than absence of an early interferon response.

This interpretation is supported by evidence that MDV-associated immune dysfunction affects both cytokine production and cellular effector activity. MDV-specific T cells can proliferate and express antiviral cytokines while showing impaired degranulation, indicating that transcriptional responses do not necessarily translate into effective cytotoxic viral clearance [17]. The MDV-induced tumor microenvironment can also suppress activation and *IFN-γ* production by tissue-resident γδ T cells (Matsuyama-Kato et al., 2023). The concurrent decline in *IL-2* may similarly indicate impaired T-cell activation, proliferation, or maintenance. [15] found no significant alteration in *IL-2* expression during early cytolytic infection, emphasizing that *IL-2* responses vary with infection phase and experimental context. Thus, reduced *IFN-γ* and *IL-2* should be interpreted as burden-associated indicators of weakened cellular immunity rather than as proven initiating mechanisms of viral replication.

In contrast, *IL-4*, *IL-6*, *IL-10*, and *IL-17* increased with viral burden. Previous studies documented induction of *IL-4*, *IL-6*, *IL-10*, IL-12, IL-13, and interferons during cytolytic MDV infection, with *IL-10* remaining elevated beyond the lytic phase [13, 15]. Cytokine expression also varies between $CD4^+$ and $CD8^+$ splenic T-cell subsets and between genetically resistant and susceptible chickens, emphasizing the importance of host background, infection timing, and cellular source [16]. The present cytokine pattern therefore supports broad immune dysregulation rather than a simple transition toward one canonical T-helper phenotype. *IL-4* may reflect Th2-associated deviation, *IL-6* may accompany inflammatory activation and tissue injury, and *IL-10* may restrain excessive inflammation while simultaneously limiting antigen presentation and antiviral effector responses.

*IL-10* showed the largest proportional increase per 10-fold rise in MDV burden. This observation is consistent with persistent *IL-10* transcription during later infection and elevated *IL-10* expression in susceptible birds and defined T-cell subsets [15, 16]. Nevertheless, causality cannot be inferred from the present cross-sectional associations. Increased *IL-10* could facilitate viral persistence through immunoregulatory suppression, arise as compensatory feedback to control tissue inflammation, or reflect expansion of regulatory or transformed lymphocyte populations. *IL-10* should therefore be regarded as a candidate burden-associated marker rather than an established causal driver of MDV progression.

The positive association between *IL-17* and MDV burden also requires careful interpretation. MDV infection induces *IL-17*A expression and increases the frequency of *IL-17*A-positive T-cell populations. However, experimental administration of recombinant chicken *IL-17*A following vaccination reduced tumor incidence under some treatment conditions, demonstrating that *IL-17*A cannot be classified as uniformly pathogenic [17]. Its effects may vary according to timing, magnitude, cellular

source, vaccination status, and the surrounding cytokine environment. Increased *IL-17* expression in higher-burden birds may therefore reflect inflammatory tissue responses, an attempt to strengthen antiviral immunity, or an ineffective compensatory response rather than a direct mechanism of disease progression.

Although tissue-specific correlations appeared broader in the liver, the mixed-effects interaction analysis did not confirm significantly different viral burden–cytokine slopes between liver and spleen. This may reflect limited statistical power or greater splenic cellular heterogeneity, where infected B cells, activated T cells, latently infected $CD4^+$ cells, antigen-presenting cells, and transformed lymphocytes may coexist. Cytokine-expression studies in sorted splenic lymphocyte populations have demonstrated substantial temporal and cell-subset-specific variation during MDV infection [16]. The heatmap in the present study similarly demonstrated considerable interindividual and within-bird variation. Such heterogeneity is expected in naturally affected field chickens, in which infection timing, circulating viral strain, host genetics, nutritional condition, coinfections, and lesion distribution are not experimentally synchronized.

The study has several strengths, including the use of paired liver and spleen samples, direct quantification of MDV burden, and integrated assessment of multiple cytokines within the same birds. These features enabled tissue-aware analysis of virus–host relationships under natural field conditions. The cross-sectional design precluded causal and temporal inference. Although the sample size provided adequate power for most observed cytokine associations, it may have limited the detection of weaker effects and tissue-specific interactions. Viral burden was normalized to DNA mass, cytokine expression relied on a single reference gene, and transcript-level findings were not confirmed at the protein or functional level. Control birds originated from a different source, and infection stage, viral pathotype, and possible coinfections were not fully characterized. Future studies incorporating longitudinal sampling, histopathology, host-cell-normalized qPCR, viral oncogene analysis, cytokine protein measurement, and cell-specific immune profiling would further validate and extend these findings.

Overall, the findings support a model in which increasing systemic MDV burden is accompanied by reduced *IFN-γ*- and *IL-2*-associated cellular immunity and enhanced *IL-4*, *IL-6*, *IL-10*, and *IL-17* responses. The combined cytokine profile is biologically more informative than any individual transcript and may provide a basis for developing composite indicators of MDV burden and disease progression. Such markers, however, require validation in independent chicken populations and against clinically meaningful outcomes, including lymphoma severity, mortality, and longitudinal progression.

## Materials and methods

# Ethics approval

The study protocol was reviewed and approved by the Animal Ethics Committee of Chattogram Veterinary and Animal Sciences University, Chattogram, Bangladesh (Approval No. CVASU/Dir(R&E)EC/2025/952/14). All sample collection and laboratory procedures were performed in accordance with the approved protocol and relevant institutional biosafety guidelines.

# Study population and sample collection

A total of 35 unvaccinated, 26-week-old chickens clinically suspected of Marek's disease were obtained from a Zonal Poultry Farm in Chattogram, Bangladesh. The number of birds sampled reflected the availability of eligible field cases during the study period. Following molecular screening, MDV-positive birds were retained as the infected group. Birds from the suspected flock that tested negative for MDV were not considered suitable controls because they had been selected on the basis of clinical or postmortem suspicion of disease and therefore could not be regarded as healthy reference birds. Accordingly, five apparently healthy chickens obtained independently from a local market and confirmed negative for MDV by *ICP4*-targeted conventional PCR were included as controls. Following postmortem examination, approximately 100–150 mg each of liver and spleen tissue was collected aseptically from every bird using separate sterile instruments. Samples were individually labelled, transported to the laboratory in liquid nitrogen, and stored at − 80°C until nucleic-acid extraction.

# DNA and RNA extraction

Genomic DNA was extracted separately from liver and spleen tissues using the DNeasy Blood and Tissue Kit (#69504, Qiagen, Hilden, Germany) according to the manufacturer's instructions. Total RNA was extracted from liver and spleen tissues using the RNeasy Mini Kit (#74104, Qiagen, Hilden, Germany). Both DNA and RNA concentration and purity were assessed using a NanoDrop One® spectrophotometer (Thermo Fisher Scientific, USA). Extracted DNA and RNA were stored at − 80°C until further analysis.

## Complementary DNA synthesis

For all samples equal quantities (1 µg for each) of total RNA were reverse-transcribed into complementary DNA using High-Capacity cDNA Reverse Transcription Kit with RNase inhibitor (#4374966, Thermo Fisher Scientific, USA) in accordance with the manufacturer's protocol. Each reverse-transcription reaction was prepared in a final volume of 20 µL containing RNA template, reverse-transcription master mix, primer, and nuclease-free water. Reverse transcription was performed in a FlexCycler² thermal cycler (Analytik Jena, Germany) using an initial incubation at 25°C for 10 min, cDNA synthesis at 42°C for 60 min, and enzyme inactivation at 85°C for 5 min, followed by holding at 4°C. Synthesized cDNA was stored at − 20°C until analysis.

## Conventional PCR and primer validation

MDV infection was confirmed by conventional PCR targeting the *ICP4* gene. Each 25-µL reaction contained 12.5 µL of 2× GoTaq Master Mix (#M7123, Promega, WI), 0.5 µL each of forward and reverse primers, 2 µL of DNA template, and nuclease-free water. Amplification was performed using an initial denaturation at 95°C for 10 min, followed by 40 cycles of 95°C for 15 s, annealing at 55°C for 30 s, and 72°C for 30 s, with a final extension at 72°C for 5 min. Positive and negative controls were included in each run. Samples producing the expected 247-bp *ICP4* amplicon were considered MDV-positive.

Before RT-qPCR analysis, the specificity of the cytokine primers was verified using a representative synthesized cDNA sample. Amplicons for *IFN-γ, IL-2, IL-4, IL-6, IL-10, IL-17*, and *GAPDH* were purified and subjected to bidirectional Sanger sequencing (Table 1). The resulting consensus sequences were compared with reference chicken sequences using BLASTn, and primer pairs showing correct target identity were used for subsequent gene-expression analysis.

## Quantification of MDV genomic burden

MDV genomic burden in liver and spleen tissues was quantified using SYBR Green-based quantitative real-time PCR targeting the *ICP4* gene. Reactions were performed on an Applied Biosystems 7500 Fast Real-Time PCR System using Brilliant III Ultra-Fast SYBR QRT PCR MasterMix (#600882Thermo Fisher Scientific, USA). Each 20-µL reaction contained 10 µL of master mix, 0.4 µM each of forward and reverse primers, approximately 100 ng of genomic DNA, and nuclease-free water. All samples were analyzed in technical triplicate. The amplification run consisted of initial denaturation at 95°C for 10 min, followed by 40 cycles of 95°C for 15 s, primer-specific annealing at 60°C for 30 s, and extension at 72°C for 30 s. Melting-curve analysis was performed after amplification to confirm product specificity. Absolute copy numbers were estimated using a calibration curve generated from tenfold serial dilutions of a recombinant plasmid containing the *ICP4* target fragment [20]. Primer efficiency was considered acceptable when it ranged from 90% to 110%. Technical replicates showing non-specific melting profiles or amplification failure were excluded before calculation of the sample mean. Viral burden was expressed as MDV genome copies per nanogram (ng) of extracted DNA. Samples without detectable amplification were recorded as non-detectable.

## Cytokine-expression analysis

The expressions of *IFN-γ*, *IL-2*, *IL-4*, *IL-6*, *IL-10*, and *IL-17* were evaluated in paired liver and spleen samples using SYBR Green RT-qPCR. Each 20-µL reaction contained 10 µL of Brilliant III Ultra-Fast SYBR QRT PCR MasterMix (#600882, Thermo Fisher Scientific, USA), 0.4 µM each of gene-specific forward and reverse primers, approximately 100 ng of cDNA, and nuclease-free water. All reactions were conducted in technical triplicate. Thermal cycling consisted of initial activation and denaturation at 95°C for 10 min, followed by 40 cycles of 95°C for 15 s and primer-specific annealing-extension at 55–62°C for 30 s. Product specificity was evaluated using melting-curve analysis. Standard curves prepared from tenfold serial dilutions of purified target-gene amplicons were used to estimate transcript abundance. Cytokine expression was normalized to GAPDH expression to account for differences in RNA input and reverse-transcription yield [21]. The three replicates were averaged to

obtain one normalized expression value for each cytokine in each bird–tissue combination. Technical replicates were not treated as independent biological observations.

# Definition and analytical treatment of MDV burden

MDV burden was analyzed primarily as a continuous quantitative variable and expressed as viral genome copies per nanogram of extracted DNA. Because the copy-number data were right-skewed, values were $\log_{10}$-transformed before association analyses. Continuous values were retained for the primary statistical analyses to avoid loss of information associated with arbitrary categorization [22]. For descriptive comparisons only, MDV-positive birds were additionally classified into lower- and higher-burden groups using a study-specific systemic burden index. For each bird, the index was calculated as the geometric mean of the mean viral loads measured in paired liver and spleen samples:

$$Systemic\ MDV\ burden = \sqrt{mean\ liver\ MDV\ load\ \times\ \ mean\ spleen\ MDV\ load}$$

The median systemic burden among the 18 MDV-positive birds was 2,983.54 copies/ng DNA and was used as the descriptive cutoff. Birds with systemic burden values at or below the median were classified as the lower-burden group, whereas those with values above the median were classified as the higher-burden group. This median-based classification was used only to facilitate descriptive summaries and visualization and was not interpreted as representing latent or clinical stages of infection. Furthermore, the cutoff was not considered a diagnostic or biologically validated threshold. Clinical and pathological disease categories, where available, were defined independently of the measured viral burden.

# Statistical analysis

Data was compiled in Microsoft Excel 365 and analyzed in R v4.5.3 [23]. Technical qPCR replicates were inspected for amplification specificity and analytical consistency and were averaged before statistical analysis. The bird, rather than the individual qPCR well, was considered the biological unit. Viral loads in paired liver and spleen tissues were compared among MDV-positive birds using the Wilcoxon signed-rank test because the copy-number data were non-normally distributed. Grouped cytokine-expression data were summarized using boxplots, and exploratory comparisons among control, lower-burden, and higher-burden groups were performed separately for each tissue using the Kruskal–Wallis test. Associations between viral burden and cytokine expression were assessed primarily using linear mixed-effects models. For each cytokine, the mean normalized expression value was $\log_2$-transformed and modeled as the outcome. Centered $\log_{10}$-transformed MDV copies/ng DNA and tissue were included as fixed effects, and bird identity was included as a random intercept to account for paired liver and spleen observations:

$$log_2\left(Cytokine\ expression\right) = \beta_0 + \beta_1\left[log_{10}\left(MDV\ copies/ng\ DNA\right)\right] + \beta_2\left(Tissue\right) + \mu_i + \epsilon_{ij}$$

Here,

$\mu_i$ = random intercept for bird i

$\epsilon_{ij}$ = residual error for tissue j within bird i

Controls were excluded from these continuous association models because their viral-load results represented non-detection rather than quantitatively measured zero values. Viral-load effects were assessed by likelihood-ratio tests (LRT) comparing models with and without the MDV-burden term. MDV burden-by-tissue interactions were tested separately to determine whether associations differed between liver and spleen. Where the interaction was not supported, the more parsimonious common-slope model was retained. Tissue-specific associations were additionally explored using Spearman's rank correlation among MDV-positive birds. P values were adjusted using the Benjamini–Hochberg procedure to control the false discovery rate (FDR). A post hoc sensitivity analysis was performed using the effect estimates and standard errors derived from the linear mixed-effects models to evaluate sample-size adequacy. Assuming the observed effect magnitude and variance structure, approximately 18 MDV-positive birds (36 paired liver and spleen observations) were estimated to provide > 80% power (except for IL-17) at a two-sided α of 0.05 for detecting the smallest observed cytokine association (Table S1). Adjusted P values (q values) < 0.05 were considered statistically significant, and effect estimates are presented with 95% confidence intervals.

# Data availability statement

The datasets generated and analyzed during the current study, including the MDV-load and cytokine-expression data supporting the reported results, are publicly available in the Zenodo repository, https://doi.org/10.5281/zenodo.22082126. The R scripts used for statistical analysis and figure generation are also available in the GitHub repository, https://github.com/TMR367/Cytokine-Expression-in-MDV-infection. Sanger sequencing was performed solely to confirm the specificity of primers using representative amplicons from a single cDNA sample; no novel nucleotide sequence or sequencing-based expression dataset was generated.

# Declarations

### Additional Information

The authors declare no conflict of interest. All authors reviewed the final version of the manuscript and agreed to submission.


### Funding

This research was funded by University Grants Commission of Bangladesh (2023-24: LSC-19; to T.M.R.).


### Author contributions

**S.S.T., F.A.**: Conceptualization, Methodology, Investigation, Data Curation, Visualization, Writing - Review & Editing; **M.A., L.A., M.J.H.R., M.M.M., S.C.**: Investigation, Validation, Visualization, Data Curation, Writing - Review & Editing; **M.M., T.M.R.**: Supervision, Funding acquisition, Conceptualization, Formal analysis, Resources, Writing - Original Draft, Writing - Review & Editing.

# References


1. Davison, F. & Nair, V. Use of Marek's disease vaccines: could they be driving the virus to increasing virulence? *Expert Rev. Vaccines* **4**, 77–88 (2005).
2. Read, A. F. *et al.* Imperfect Vaccination Can Enhance the Transmission of Highly Virulent Pathogens. *PLoS Biol.* **13**, e1002198 (2015).
3. Calnek, B. W., Adldinger, H. K. & Kahn, D. E. Feather follicle epithelium: a source of enveloped and infectious cell-free herpesvirus from Marek's disease. *Avian Dis.* **14**, 219–233 (1970).
4. Souci, L. & Denesvre, C. Interactions between avian viruses and skin in farm birds. *Vet. Res.* **55**, 54 (2024).
5. Barrow, A. D., Burgess, S. C., Baigent, S. J., Howes, K. & Nair, V. K. Infection of macrophages by a lymphotropic herpesvirus: a new tropism for Marek's disease virus. *J. Gen. Virol.* **84**, 2635–2645 (2003).
6. Berthault, C. *et al.* Atrophy of primary lymphoid organs induced by Marek's disease virus during early infection is associated with increased apoptosis, inhibition of cell proliferation and a severe B-lymphopenia. *Vet. Res.* **49**, (2018).
7. Gamal, M. A. N., El-Nagar, E. M. S., Khattab, M. S. & Salem, H. M. Molecular discernment and histopathological features of oncogenic Marek's disease virus among different farmed avian species in Egypt. *Scientific Reports 2025 15:1* **15**, 15409- (2025).
8. Lupiani, B. *et al.* Marek's disease virus-encoded Meq gene is involved in transformation of lymphocytes but is dispensable for replication. *Proc. Natl. Acad. Sci. U. S. A.* **101**, 11815–11820 (2004).
9. Chacón, R. D. *et al.* Molecular characterization of the meq oncogene of Marek's disease virus in vaccinated Brazilian poultry farms reveals selective pressure on prevalent strains. *Vet. Q.* **44**, 1 (2024).
10. Bumstead, N., Sillibourne, J., Rennie, M., Ross, N. & Davison, F. Quantification of Marek's disease virus in chicken lymphocytes using the polymerase chain reaction with fluorescence detection. *J. Virol. Methods* **65**, 75–81 (1997).

11. Islam, A. *et al.* Differential amplification and quantitation of Marek's disease viruses using real-time polymerase chain reaction. *J. Virol. Methods* **119**, 103–113 (2004).
12. Zhang, Z., Liu, S., Ma, C., Zhao, P. & Cui, Z. Absolute quantification of a very virulent Marek's disease virus dynamic quantity and distributions in different tissues. *Poult. Sci.* **94**, 1150–1157 (2015).
13. Kaiser, P., Underwood, G. & Davison, F. Differential Cytokine Responses following Marek's Disease Virus Infection of Chickens Differing in Resistance to Marek's Disease. *J. Virol.* **77**, 762 (2003).
14. Bertzbach, L. D. *et al.* IFNα and IFNγ Impede Marek's Disease Progression. *Viruses 2019, Vol. 11, Page 1103* **11**, 1103 (2019).
15. Heidari, M., Zhang, H. M. & Sharif, S. Marek's disease virus induces Th-2 activity during cytolytic infection. *Viral Immunol.* **21**, 203–213 (2008).
16. Parvizi, P., Read, L., Abdul-Careem, M. F., Lusty, C. & Sharif, S. Cytokine gene expression in splenic CD4(+) and CD8(+) T-cell subsets of chickens infected with Marek's disease virus. *Viral Immunol.* **22**, 31–37 (2009).
17. Boodhoo, N. & Behboudi, S. Marek's disease virus-specific T cells proliferate, express antiviral cytokines but have impaired degranulation response. *Front. Immunol.* **13**, 973762 (2022).
18. Abdul-Careem, M. F., Read, L. R., Parvizi, P., Thanthrige-Don, N. & Sharif, S. Marek's disease virus-induced expression of cytokine genes in feathers of genetically defined chickens. *Dev. Comp. Immunol.* **33**, 618–623 (2009).
19. Matsuyama-Kato, A. *et al.* The tumor microenvironment generated by Marek's disease virus suppresses interferon-gamma-producing gamma delta T cells. *Vet. Microbiol.* **285**, (2023).
20. Akter, L. *et al.* Investigation of koala retrovirus in captive koalas with pneumonia and comparative analysis of subtype distribution. *Arch. Virol.* **168**, (2023).
21. Akter, L. *et al.* Elevated oncogene expressions in koala infected with multiple koala retrovirus subtypes: a preliminary study. *Virus Genes* **61**, 629–633 (2025).
22. Altman, D. G. & Royston, P. The cost of dichotomising continuous variables. *BMJ* **332**, 1080 (2006).
23. R Core Team. R: A language and environment for statistical computing. R Foundation for Statistical Computing, Vienna, Austria. *URL: https://www.R-project.org/* (2020).
24. Kalyani, I. H. *et al.* Characterization of the ICP4 gene in pathogenic Marek's disease virus of poultry in Gujarat, India, using PCR and sequencing. *Vet. Arh.* **80**, 683–692 (2010).
25. Motai, Y. *et al.* Virulence of Marek's disease virus in Japan is linked to polymorphisms in the meq oncogene. *J. Gen. Virol.* **107**, 002232 (2026).
26. Huo, S. *et al.* Co-Expression of Chicken IL-2 and IL-7 Enhances the Immunogenicity and Protective Efficacy of a VP2-Expressing DNA Vaccine against IBDV in Chickens. *Viruses* **11**, 476 (2019).
27. Tan, F. *et al.* Immune synergistic mechanism of recombinant plasmid adjuvant containing chicken IL-4 and IL-2 fusion genes on chicken coccidia live vaccine. *Poult. Sci.* **103**, 103204 (2024).
28. Matsuyama-Kato, A. *et al.* Activated Chicken Gamma Delta T Cells Are Involved in Protective Immunity against Marek's Disease. *Viruses* **15**, 285 (2023).

## Tables

**Table 1:** Characteristics of primers used in the study.

| Target | Primer name | Sequences (5′–3′) | Annealing Temperature ($T_a$) | Amplicon size (bp) | NCBI Reference sequence ID | References |
|---|---|---|---|---|---|---|
| *ICP4* (PCR) | MDV-F | GGATCGCCCACCACGATTACTACC | 55 °C | 247 | AY362726 | [24] |
| | MDV-R | ACTGCCTCACACAACCTCATCTCC | | | | |
| *ICP4* (qPCR) | MDV-1 F | GCA TCG ACA AGC ACT TAC GG | 60 °C | 128 | AY362726 | [25] |
| | MDV-1 R | CGA GAG CGT CGT ATT GTT TGG | | | | |
| *IL-2* | chIL2S-F | ACTCTGCAGTGTTACCTGGG | 56 °C | 151 | AF000631.1 | [26] |
| | chIL2S-R | TGCATTCACTTCCGTGTGA | | | | |
| *IL-4* | chIL4S-F | AGCCAGCACTGCCACAAGAAC | 58 °C | 156 | NM-001007079.1 | [27] |
| | chIL4S-R | GTGGAAGAAGGTACGTAGGTCTGC | | | | |
| *IL-6* | chIL6-F | CGGCTTCGACGAGGAGAAAT | 62 °C | 188 | NM_204628.2 | This study |
| | chIL6-R | GGATGACCACTTCATCGGGA | | | | |
| *IL-10* | chIL10-F | GGGAGCTGAGGGTGAAGTTTGAGGA | 58 °C | 200 | AJ621254.1 | This study |
| | chIl10-R | CTGCTGATGACTGGTGCTGGTCTG | | | | |
| *IL-17* | chIL17-F | TATCAGCAAACGCTCACTGG | 58 °C | 110 | NM_204460.2 | [28] |
| | chIL17-R | AGTTCACGCACCTGGAATG | | | | |
| IFN- γ | chIFNG-F | CCAAGCTCCCGATGAACGA | 58 °C | 163 | NM_205149.2 | This study |
| | chIFNG-R | AGTTGAGCACAGGAGGTCATA | | | | |
| GAPDH | chGAPDH-F | TGCTGCCCAGAACATCATCC | 56-62 °C | 142 | NM_204305.2 | This study |
| | chGAPDH-R | ACGGCAGGTCAGGTCAACAA | | | | |

**Table 2.** Mixed-effects model estimates for association between MDV burden and cytokine expression in paired liver and spleen samples.

| Cytokine | Fold change per 10-fold increase in MDV | 95% CI | BH-adjusted q | Interpretation |
|---|---|---|---|---|
| ***IFN-γ*** | 0.817 | 0.727–0.918 | 0.0018 | 18.3% lower expression |
| ***IL-2*** | 0.837 | 0.775–0.904 | 0.0004 | 16.3% lower expression |
| ***IL-4*** | 1.372 | 1.139–1.653 | 0.0018 | 37.2% higher expression |
| ***IL-6*** | 1.247 | 1.089–1.429 | 0.0018 | 24.7% higher expression |
| ***IL-10*** | 1.527 | 1.230–1.896 | 0.0012 | 52.7% higher expression |
| ***IL-17*** | 1.319 | 1.072–1.624 | 0.0123 | 31.9% higher expression |

# Figures

**Figure 1**

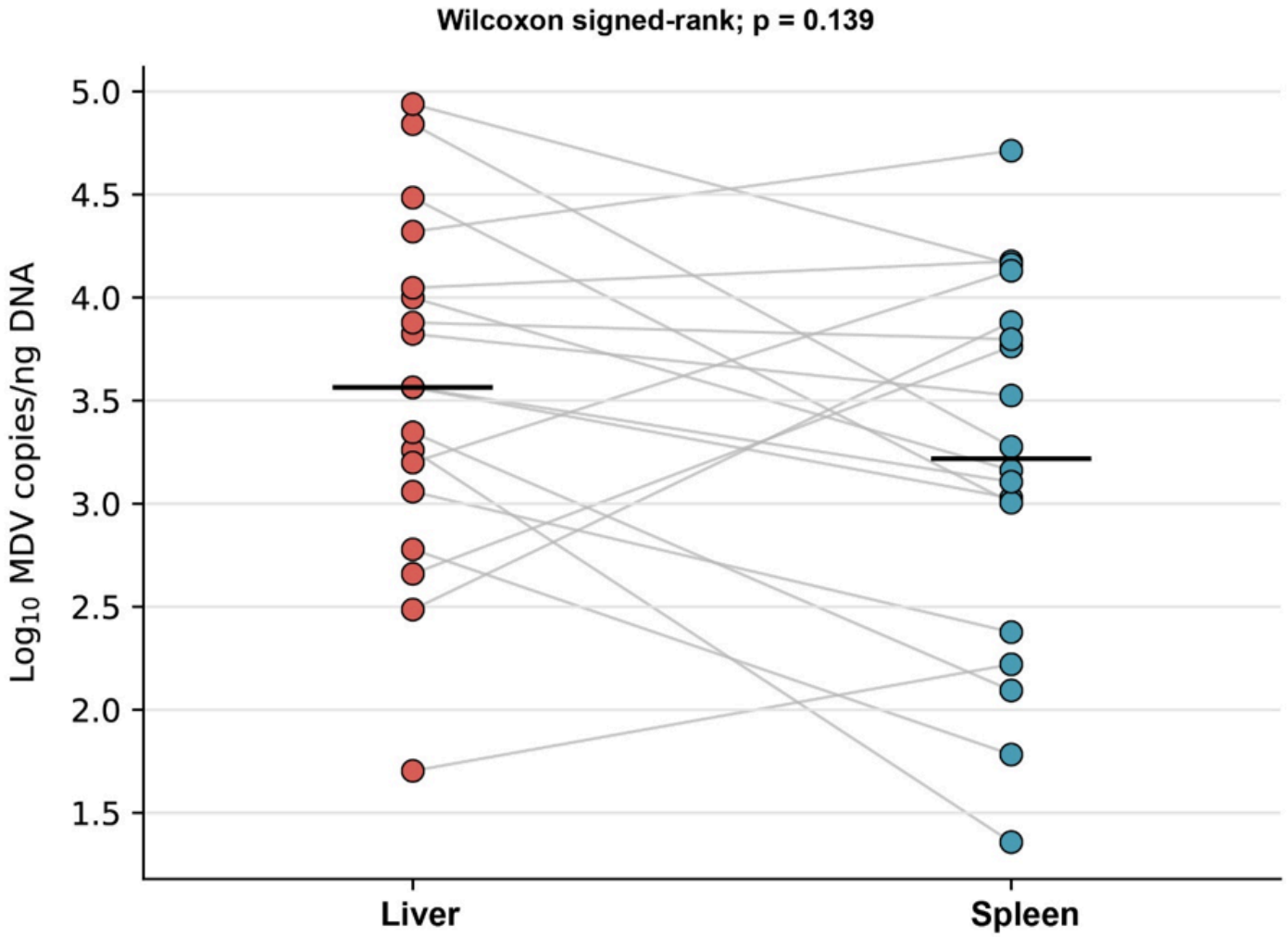



**Figure 1**

Paired comparison of Marek's disease virus burden in liver and spleen. Mean MDV genomic burden was calculated from three replicate qPCR observations for each tissue and expressed as genome copies per nanogram of extracted DNA. Points represent individual MDV-positive birds, and lines connect paired liver and spleen samples from the same bird. Viral-load values are presented on a $\log_{10}$ scale. Paired liver and spleen burdens were compared using the Wilcoxon signed-rank test among the 18 MDV-positive birds.

**Figure 2**

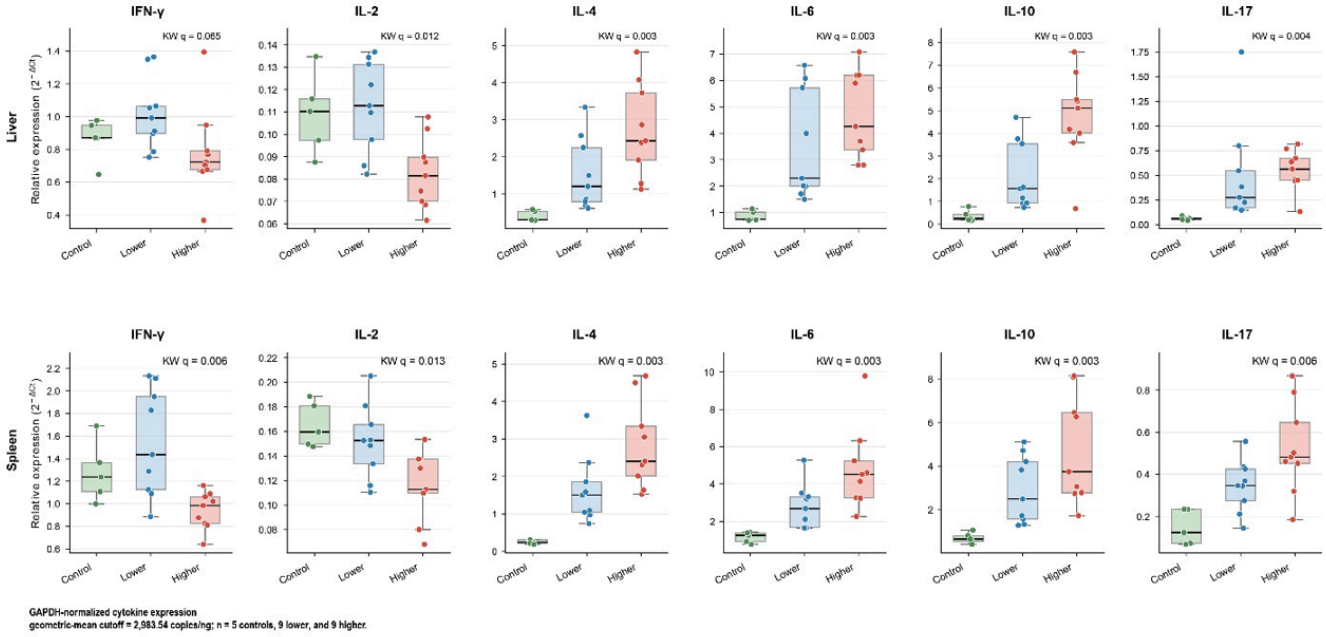



**Figure 2**

GAPDH-normalized cytokine expression according to systemic MDV-burden category. Relative expressions of *IFN-γ*, *IL-2*, *IL-4*, *IL-6*, *IL-10*, and *IL-17* in paired liver and spleen samples from MDV-negative controls and MDV-positive birds classified as having lower or higher systemic burden. The bird-level systemic burden index was calculated as the geometric mean of paired liver and spleen MDV loads. MDV-positive birds were divided descriptively using the study-specific median cutoff of 2,983.54 copies/ng DNA, resulting in nine lower-burden and nine higher-burden birds. Boxes indicate the interquartile range, horizontal lines represent medians, whiskers show the data range within the plotting rule, and points represent individual birds. Overall group differences were evaluated separately for each tissue and cytokine using the Kruskal–Wallis test, with Benjamini–Hochberg-adjusted q-values shown. These burden categories were used only for descriptive presentation and were not interpreted as diagnostic or disease-stage thresholds.

**Figure 3**

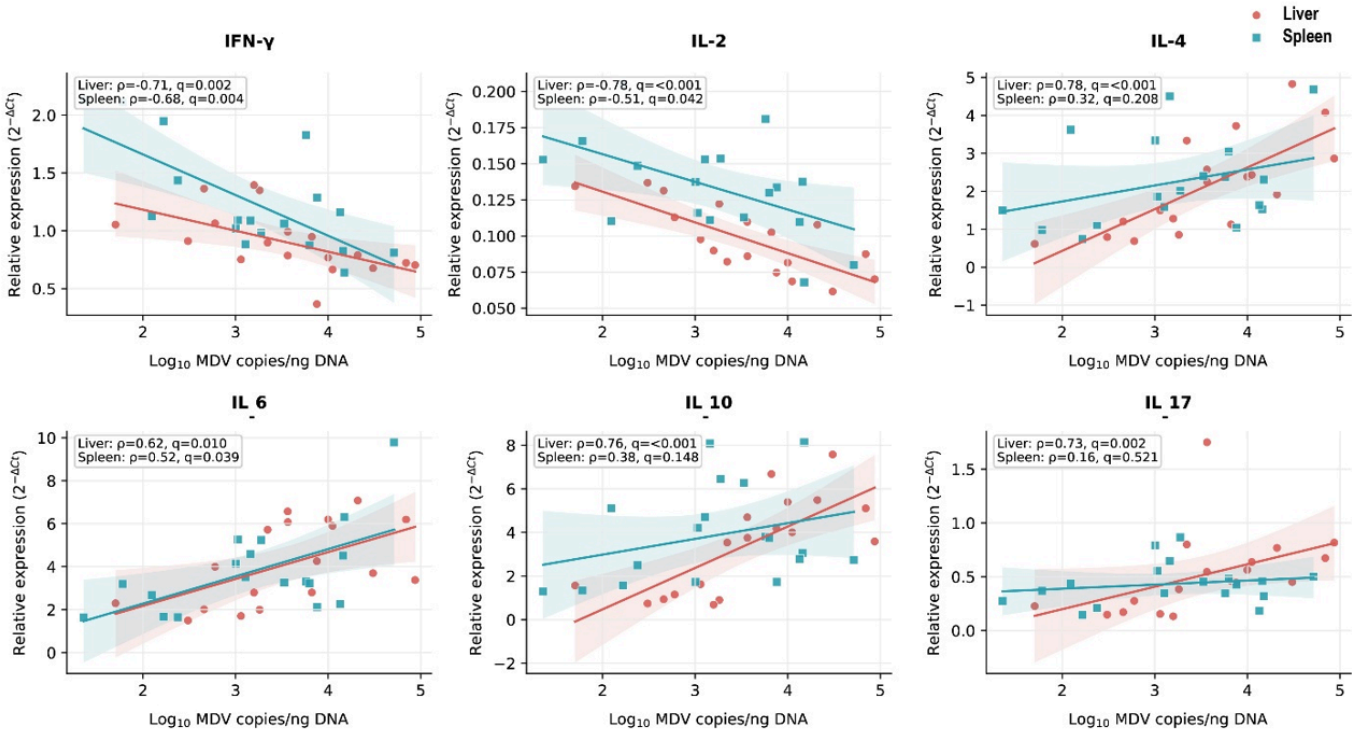



**Figure 3**

Tissue-specific associations between MDV burden and cytokine expression. Relationships between continuous $\log_{10}$-transformed MDV burden and GAPDH-normalized expression of *IFN-γ*, *IL-2*, *IL-4*, *IL-6*, *IL-10*, and *IL-17* in liver and spleen samples from MDV-positive birds. Each point represents one bird–tissue observation. Lines illustrate tissue-specific fitted trends for visualization. Spearman's rank correlation coefficients and corresponding P-values or multiple-testing-adjusted q-values are presented for each tissue. Controls were excluded because MDV was non-detectable rather than quantitatively measured as zero.

**Figure 4**

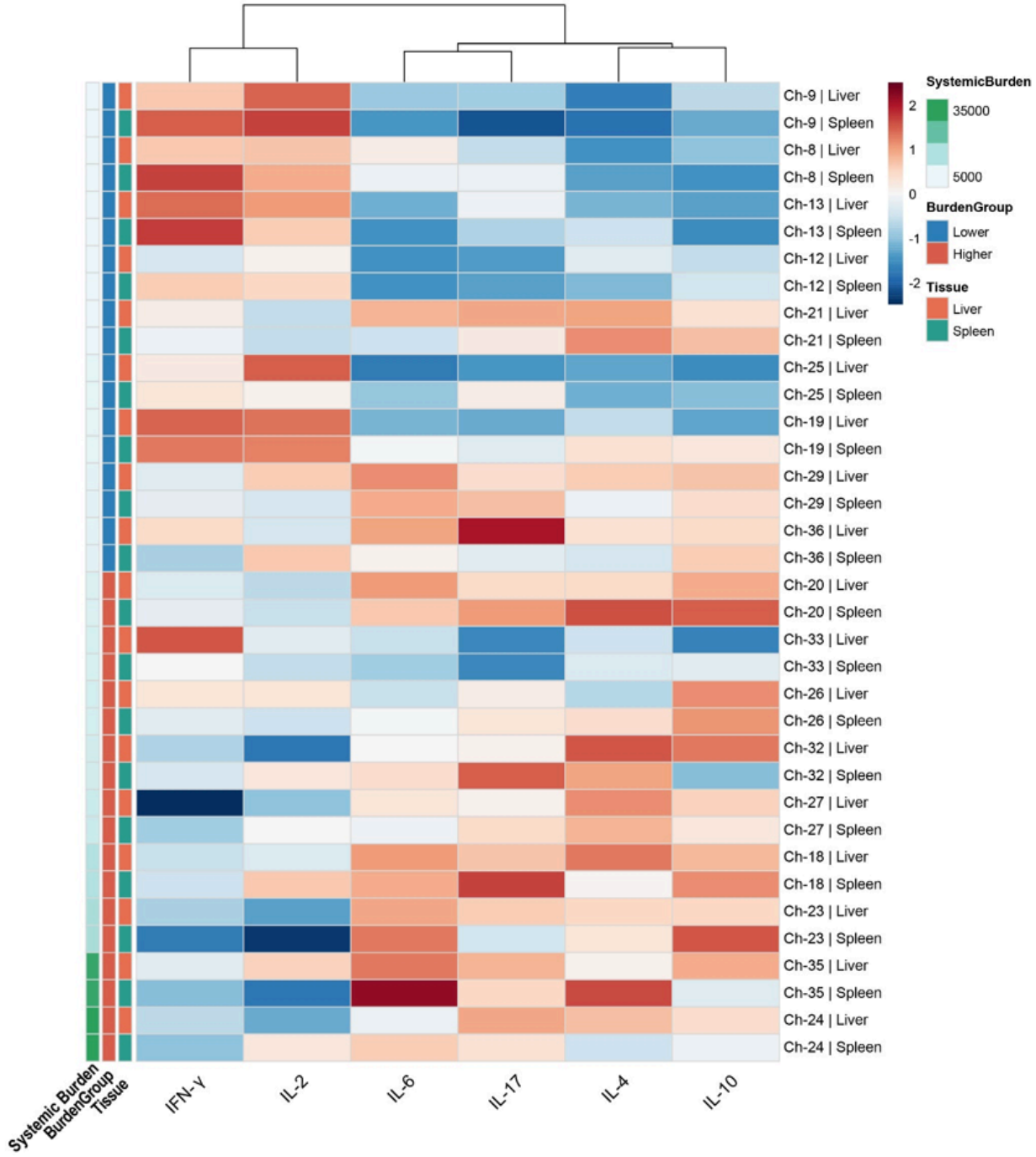



**Figure 4**

Tissue-resolved heatmap of cytokine-expression profiles in MDV-positive chickens. Heatmap showing standardized expression patterns of *IFN-γ*, *IL-2*, *IL-4*, *IL-6*, *IL-10*, and *IL-17* in paired liver and spleen samples. Expression values were standardized within each cytokine–tissue combination and displayed as row- or column-scaled z-scores, with warmer shades indicating relatively higher expression and cooler shades indicating relatively lower expression. Birds were ordered according to increasing systemic MDV burden, while clustering illustrates similarities among cytokines and individual expression profiles. Liver and spleen observations were retained separately to preserve tissue-specific variation.

**Figure 5**

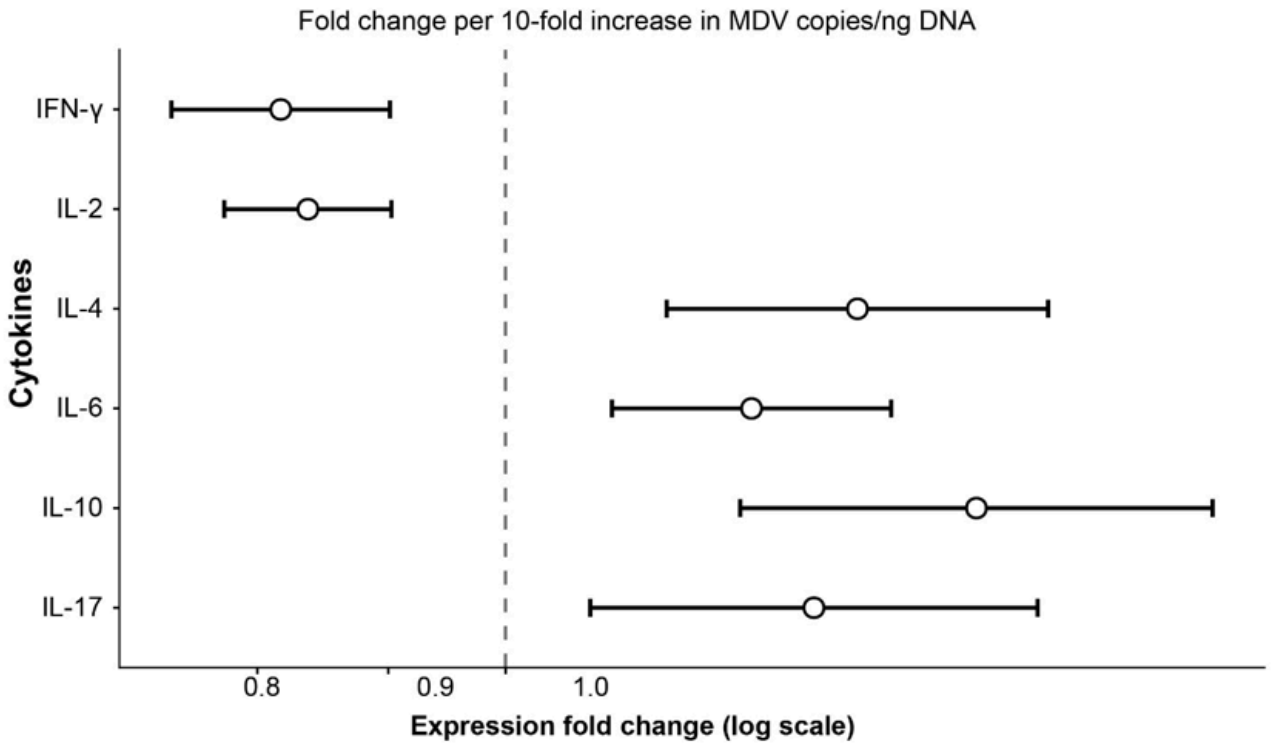



**Figure 5**

Mixed-effects model estimates of cytokine associations with MDV burden. Forest plot shows fold changes in GAPDH-normalized cytokine expression associated with each 10-fold increase in MDV copies/ng DNA. Separate linear mixed-effects models were fitted for *IFN-γ*, *IL-2*, *IL-4*, *IL-6*, *IL-10*, and *IL-17* using $\log_2$-transformed cytokine expression as the outcome, continuous $\log_{10}$ MDV burden and tissue as fixed effects, and bird identity as a random intercept. Points represent estimated fold changes, and horizontal bars indicate 95% confidence intervals. The vertical reference line at 1.0 denotes no association. Values below 1 indicate decreasing expression, whereas values above 1 indicate increasing expression with greater viral burden. Statistical significance was evaluated using likelihood-ratio tests with Benjamini–Hochberg correction across the six cytokines.

## Supplementary Files

This is a list of supplementary files associated with this preprint. Click to download.

- SupplementaryMaterials.docx